RSC Advances

ROYAL SOCIETY OF CHEMISTRY

www.rsc.org/advances

Nano-micro Structure of Functionalized Boron Nitride and Aluminum Oxide for Epoxy Composites with Enhanced Thermal Conductivity and Breakdown Strength

Lijun Fang[a], Chao Wu[a], Rong Qian[a], Liyuan Xie[a], Ke Yang[a], Pingkai Jiang[a,b,*]

a. Shanghai Key Lab of Electrical Insulation and Thermal Aging, Shanghai Jiao Tong University, 800 Dongchuan Road, Shanghai 200240, P. R. China

b. Shanghai Engineering Center for Material Safety of Nuclear Power Equipment, 2548 Pudong Road, Shanghai 200240, P. R. China

*Corresponding author: Fax/Tel, +86-021-54740787; E-mail, pkjiang@sjtu.edu.cn

Abstract

Polymer-based composites with high thermal conductivity and breakdown strength are increasingly desirable in both electronic and electric industry. Herein, we`ve designed a nano-micro structure of 2-D micro-scale hexagonal boron nitride (*h*-BN) and 0-D nano-scale α-alumina (α-Al_2O_3) hybrid fillers for epoxy composites with high thermal conductivity and breakdown strength. So as to improve interface interaction, both fillers are functionalized with hyperbranched aromatic polyamide (HBP). It is found that both structure design and surface modification play important roles. Surface modification can enhance many physical properties of composites, such as thermal conductivity, thermal stability and breakdown strength. Importantly, nano-micro structure presents noticeable synergistic effect on both thermal conductivity and ac breakdown strength. The obtained composite with 26.5 vol% fillers presents high thermal conductivity of 0.808 W m^{-1} K^{-1} (4.3 times that of epoxy). In addition, the breakdown strength of composite at 4.4 vol% content is up to 40.55 kv mm^{-1}, 21.5% higher than that of neat epoxy (33.38 kv mm^{-1}).

Introduction

Polymer composites, combining the merits of both polymer matrix and filler component, have attracted increasing research interest in the field of electronic device and electrical equipment due to good comprehensive properties, feasible processability and low cost[1]. However, common polymer materials are thermally insulating and can`t meet the need of heat dissipation for accelerated minimization and integration of chip components[2].

Currently, two methods are taken to improve thermal conductivity. One is introducing electrically conductive inclusions (e.g., graphene[3], carbon nanotube[4], graphite[5]) with high intrinsic thermal conductivity into matrix. Though these fillers can notably increase thermal conductivity at low content, breakdown strength are sharply reduced since they inevitably cause target composites electrically conductive[6]. Alternative method is using electrically insulating ceramic fillers (e.g., BN[7, 8], AlN[9], Al_2O_3[10]) which are able to withstand high electric fields. However, so as to obtain favorable thermal conductivity, high loadings (> 50 vol%) are usually required, which in return deteriorates mechanical and processing properties[11, 12]. On the other hand, the addition of these fillers always reduce breakdown strength of resulting composites due to weak interface[13]. Therefore, the fabrication of composites with high thermal conductivity and breakdown strength at low filler content is still a challenge.

For this target, we design a nano-micro structure of 2-D and 0-D ceramic fillers for epoxy composites with enhanced thermal conductivity and breakdown strength. 2-D micro-scale hexagonal boron nitride (h-BN) platelet is chosen owing to high thermal conductivity of 390 W m^{-1} K^{-1} in basal plane, ultrahigh breakdown strength of 794 MV mm^{-1} and large aspect ratio[14, 15]. The 2-D structure and intrinsic properties qualify BN platelet as a promising candidate to prepare polymer-based insulating composites with high thermal conductivity. However, there exists high thermal resistance between boron nitride platelets in epoxy matrix. Therefore, another 0-D nano-scale α-alumina (α-Al_2O_3) particles with insulating property and high thermal conductivity are introduced. The role of Al_2O_3 nanoparticles is to serve as linking bridges to connect BN platelets for building a more compactible 3-D thermal conductive network. Moreover, as interface is crucial to physical properties of composites[16, 17], hyperbranched aromatic polyamide (HBP) is grafted onto surfaces of both BN and Al_2O_3 to achieve desirable dispersion and strong interface interaction[18].

In this work, we first functionalized both BN and Al2O3 with HBP via a two-step treatment. Then, a series of composites with individual or hybrid modified BN/Al_2O_3 were fabricated by blending-desolvation-curing method. Then, the influence of interface and nano-micro structure on thermal and dielectric properties was investigated. Epoxy

composites with enhanced thermal conductivity and breakdown strength were obtained at low content through surface modification and structure design. To our best knowledge, thermal and dielectric properties of epoxy composites with a hybrid of 2-D micro-scale and 0-D nano-scale modified fillers have rarely been systematically studied.

1. Experimental

1.1 Materials

Hexagonal boron nitride (*h*-BN) platelets with an average diameter of 3 μm, *α*-alumina (*α*-Al_2O_3) particles with an average diameter of 30 nm were bought from ESK Ceramics GmbH Co., Germany and Kaier Nano, China, separately. *γ*-aminopropyl-triethoxysilane (*γ*-APS) as the coupling agent was purchased from GE Silicones. The grafting monomer, 3,5-diaminobenzoic acid (DABA, Tokyo Chemical Industry Co., Japan) was purified by recrystallization from water and dried in a vacuum oven at 80 °C for 9 h. Cycloaliphatic epoxy (6105, DOW Chemicals, USA) was applied as matrix. Methyl tetrahydrophthalic anhydride (MTHPA) used as hardener and tris(dimethylaminomethyl) phenol (DMP-30) as latent catalyst were both acquired from Lunliqi Chemical Materials, China. Lithium chloride (LiCl) was dried at 230 °C overnight before applying. Other solvents, such as N-methyl-2-pyrrolidone (NMP), N,N-dimethylformamide (DMF), triphenyl phosphate (TPP), dimethylbenzene (DMB), pyridine, and methanol were analytical grade provided by Sinopharm Chemical Reagent co., Ltd, China and used without further purification.

1.2 Surface modification of BN and Al_2O_3 with silane coupling agent

Prior to silane modification, as received *h*-BN powder was dried in a vacuum oven at 180 °C for 24 h to remove absorbed moisture. In a typical experiment, 2 g BN and an appropriate amount of *γ*-APS (0.5-1 wt%) were first dispersed in 100 ml DMB. Then, the mixture was refluxed at 110-120 °C for at least 4 h. After filtration, the silane treated BN platelets were acquired and washed 3 times with DMB to remove residual siloxane moieties. The product was dried at 120 °C to constant weight and denoted as BN-APS. Al_2O_3 was silanized with *γ*-APS by the same method above and denoted as Al_2O_3-APS.

1.3 Grafting of hyperbranched aromatic polyamide from BN and Al_2O_3

In a flask, 0.76 g BN-APS and 0.76 g DABA were added into 10 mL NMP and stirred until DABA was dissolved. Then, 2.5 mL pyridine and 2.5 mL TPP as dehydrant were charged into the flask. The mixture was heated to 100 °C and stirred for 3 h under N_2. After cooling to ambient temperature, the solution was poured into 50 mL methanol to precipitate polymer. The suspended substance was collected by filtration and purified by re-precipitation from DMF into methanol with 0.1 wt% LiCl. Hyperbranched aromatic polyamide grafted BN platelets (denoted as BN-HBP) were washed with methanol and finally dried in a vacuum oven at 90 °C overnight. Al_2O_3-APS particles were treated by the same method and denoted as Al_2O_3-HBP in the following text.

1.4 Fabrication of epoxy nanocomposites

Epoxy composites were prepared as follows. Firstly, epoxy resin was mixed with latent catalyst (DMP-30, 0.5 wt%) at 80 °C by sonication and cooled down. Secondly, desired amount of fillers were dispersed in acetone (0.1 g in 5 mL) by sonication for 1 h and added into pretreated epoxy resin. The mixture was stirred at 60 °C for 1 h and sonicated for another 0.5 h to remove solvent and ensure homogeneity. Thirdly, MTHPA (80 wt% of epoxy resin) was charged in under stirring and degassed for 30 min. Finally, mixture above was poured onto stainless steel molds and pre-cured at 135 °C for 2 h followed by post-cure at 165 °C for 14 h. Samples were acquired from models after cooling to room temperature. The preparation process is illustrated in **Fig. 1.**

1.5 Characterization

Fourier-transform infrared spectrometry (FT-IR) was conducted using a Perkin-Elmer Paragon 1000 over the range of 4000-400 cm^{-1}. Thermal gravimetric analysis (TGA) was recorded with a TG-209 F3 instrument (NETZSCH, Germany) at a heating rate of 20 °C min^{-1} under nitrogen. Field emission scanning electron microscopy (FE-SEM, JSM-7401F, JEOL ltd., Japan) was used to observe distribution of fillers in composites and fractured surfaces were sputtered with a layer of gold to avoid charge accumulation. Transmission electron microscopy (TEM, JEM-2100, JEOL ltd., Japan) was performed

to observe surface structure of two fillers and their dispersion in composites. The filler sample was prepared by dropping sample solution onto ultra-thin carbon coated copper grid and air-dried. The composite specimen with thickness ca. 70 nm was trimmed by a microtome machine. Thermal diffusivity (δ, $mm^2\ s^{-1}$) was measured with LFA 447 Nanoflash (NETZSCH, Germany) on cylindrical samples (1-2 mm thick, 12.6 mm in diameter). Specific heat (C_p, $J\ g^{-1}\ K^{-1}$) was determined by DSC (200 F3, NETZSCH, Germany) and bulk density (ρ, $g\ cm^{-3}$) was determined by water displacement method. Three samples were tested for one filler content and thermal conductivity (λ, $W\ m^{-1}\ K^{-1}$) was calculated by equation:

$$\lambda = \delta \times C_p \times \rho \quad (1)$$

Breakdown strength was recorded by an AHDZ-10/100 dielectric breakdown equipment (Shanghai, Lanpotronics, China) according to ASTM D149-2004 criterion. Rectangle specimen with a thickness of 1000±50 μm was placed between two 10-mm-diameter copper ball electrodes in silicon oil at 25 °C. Then, a 50 Hz alternating voltage was used and increases at a rate of 2 $kV\ s^{-1}$ until breakdown. Dielectric property was measured by Aglient 4294A impedance analyzer with 16451B fixture (Aglient Technologies, USA) over frequency range of 10^3-10^7 Hz at room temperature. Samples with a diameter of 12.6 mm were evaporated with a thin gold layer on both surfaces to serve as electrodes.

2. Results and discussion

2.1 Characterization of hyperbranched aromatic polyamide grafted BN and Al_2O_3

FT-IR spectra of BN, BN-HBP, Al_2O_3 and Al_2O_3-HBP are shown in **Fig. 2**. In case of as received BN, strong absorption at 1374 cm^{-1} and peak at 817 cm^{-1} can be attributed to B-N stretching and bending vibration, respectively. For BN-HBP, amino groups serving as initiator sites were first introduced onto the surface of BN by treatment with γ-APS and hyperbranched aromatic polyamide was then grafted. Thereby, C-H asymmetric and symmetric stretching vibrations of γ-APS are observed at 2922 and 2856 cm^{-1}. Amide C=O stretching and characteristic of aromatic structure also appear as peaks at 1636, 1536 cm^{-1} and peak at 1605 cm^{-1}, separately. Besides, superimposition of N-H and -OH stretching vibrations causes a broad band around 3420 cm^{-1}[19]. These changes in FT-IR

spectra indicate the successful grafting of BN with hyperbranched aromatic polyamide. For as received Al_2O_3, strong absorption at 3200-3500 cm^{-1} and peak at 1630 cm^{-1} are assigned to -OH stretching and bending vibrations. In case of Al_2O_3-HBP, differences are detected: (1) C-H asymmetric and symmetric vibrations of γ-APS show at 2926 and 2850 cm^{-1}; (2) amide C=O stretching vibration emerges as peaks at 1654 and 1546 cm^{-1}; (3) feature peaks of aromatic structure are present at 1606 and 1452 cm^{-1}. To conclude, Al_2O_3 particles are functionalized with HBP as well.

TGA curves of BN, BN-HBP, Al_2O_3 and Al_2O_3-HBP measured under N_2 provide another evidence for successful wrapping of HBP. As presented in **Fig. 3**, weight losses come in the order of BN < BN-HBP and Al_2O_3 < Al_2O_3-HBP at 800 °C. In contrast to as received BN and Al_2O_3 where no significant losses appear, BN-HBP and Al_2O_3-HBP present 3.88% and 16.64% mass loss, respectively, suggesting hyperbranched aromatic polyamide is attached to surfaces of both BN and Al_2O_3. Weight grafting ratio (*Gr*) is further calculated by equation[20]:

$$Gr = \frac{W_{filler-HBP,800}}{100-W_{filler-HBP,100}} - \frac{W_{filler,800}}{100-W_{filler,100}} \quad (2)$$

Where $W_{filler\text{-}HBP,T}$ and $W_{filler,T}$ are mass losses of filler-HBP and untreated filler between 100 °C and temperature *T*. *Gr* values of BN-HBP and Al_2O_3-HBP are measured to be 4.0 and 14.2 wt%, respectively, and applied to determine volume fraction of fillers. The value of *Gr* for BN-HBP is lower than that of Al_2O_3-HBP and this can be explained by the inadequacy of functional groups on basal planes of crystal BN. Only edge planes of *h*-BN do have hydroxyl and amino groups for chemical bonding[21].

Transmission electron microscopy (TEM) is also conducted for the characterization of fillers. Before modification, BN platelets can easily aggregate owing to π-π stacking between basal planes, while Al_2O_3 particles are also inclined to agglomerate due to high surface energy and hydrogen bonds formed between existing hydroxyl groups (**Fig. S1**). Under such condition, fillers will disperse in matrix weakly, which in return diminishes properties of resulting composites. Thus, suitable tailor of surface chemistry is critical. After a two-step modification, both BN-HBP and Al_2O_3-HBP show a thin polymer layer with several nanometers in thickness as pointed out by arrows in **Fig. 4**. Herein, the

grafting of HBP is further confirmed. The introduction of peripheral amino groups is conducive to form strong covalent interface between fillers and matrix via ring-opening reaction during curing process. After surface treatment, both BN-HBP and Al_2O_3-HBP exhibit desirable dispersion and compatibility in epoxy composites (**Fig. S2**).

2.2 Morphology of neat epoxy and corresponding nanocomposites

As presented in **Fig. 5**, fracture surfaces of neat epoxy and its composite are studied by scanning electronic microscopy (SEM). For neat epoxy, fractured path with river pattern is observed in **Fig. 5a** and the direction of crack propagation is indicated by an arrow. The fracture surface is smooth, indicating a brittle fracture[22]. However, the composite with 10 wt% hybrid fillers of BN-HBP and Al_2O_3-HBP fails in brittle manner with a rough surface (**Fig. 5b**). This result can be explained by crack deflection mechanism, since the addition of fillers can lead to shear yielding or twisting of crack fronts[23]. In spite of rough surface, both fillers show desirable dispersion and homogeneity in matrix. Flaky BN-HBP (arrows marked) are coated by epoxy with no obvious naked platelets or voids present, whereas granular Al_2O_3-HBP are finely distributed with no large clusters. Such good compatibility suggests the formation of covalent bondings between amino groups of filler and epoxide groups in the matrix. Besides, from the enlarged view of framed region, considerable amounts of Al_2O_3-HBP particles are seen to locate between isolated BN-HBP platelets and serve as bridges. This kind of nano-micro structure is conducive to form a more effieient 3-D heat dissipative network[24]. This is further investigated and proved by TEM characterization in the following text.

2.3 Thermal properties of epoxy nanocomposites

Thermal conductivity of epoxy composites is determined by laser flash method at 25 $^{\circ}$C and studied as a function of BN-HBP (or BN) ratio in hybrid fillers at various contents. As presented in **Fig. 6**, two groups of composites were fabricated with as received and modified fillers at 10 wt% content. Among the former, Epoxy/Al_2O_3 presents the lowest thermal conductivity of 0.194 W m^{-1} K^{-1}, slightly higher than epoxy of 0.186 W m^{-1} K^{-1}. With the increase of BN ratio in hybrid fillers, thermal conductivity follows an inverted

"V" trend with a peak value of 0.237 W m^{-1} K^{-1} achieved when BN accounts for 80 wt%. Similar tendency is also observed for the group with modified fillers. Epoxy/Al_2O_3-HBP presents a relatively low thermal conductivity of 0.213 W m^{-1} K^{-1}, whereas a summit of 0.305 W m^{-1} K^{-1} is obtained at 4:1 mass ratio of BN-HBP/Al_2O_3-HBP. By comparison between the two groups, it`s found that composites with treated inclusions show higher thermal conductivity at the same filler ratio. This can be ascribed to two factors. Firstly, the tailor of surface chemistry improves compatibility of fillers and conduces to a better dispersion. Secondly, strong covalent interface formed between modified fillers and the matrix can reduce phonon scattering[25].

With such understanding, we further prepared epoxy composites with 30 and 50 wt% modified fillers. Similar to 10 wt% loaded groups above, thermal conductivity increases first and then decreases. And optimal quantity ratio of BN-HBP/Al_2O_3-HBP remains at 4:1 with no alteration at different contents. For convenience, composites at this ratio are denoted as **Epoxy/BA-HBP(4:1)** in other tests below. For 50 wt% composites, a peak value of 0.808 W m^{-1} K^{-1} is achieved, which is 334.4% higher than that of neat epoxy as presented in **Fig. 6b**. From thermal conductivity, we see noticeable synergistic behavior for composites with hybrid fillers. And this synergism may originate from two factors as illustrated in **Fig. 7**: (1) in nano-micro fillers, Al_2O_3-HBP particles intercalate between BN-HBP platelets and serve as physical barriers to hinder isolated BN-HBP from stacking in blending and curing processes; (2) Al_2O_3-HBP particles act as bridges for separated BN-HBP platelets, which improves the interconnectivity within 3-D heat conductive network. To further examine this synergistic effect, TEM is conducted for Epoxy/BA-HBP(4:1) at 10 wt% content. As shown in **Fig. 8**, though ruptures caused by anisotropically distributed BN-HBP during slicing process are observed, both fillers are finely dispersed in epoxy matrix with no large aggregates. And Al_2O_3-HBP particles can be seen to serve as bridges between isolated BN-HBP platelets from the enlarged view. Therefore, our assumption for synergistic effect is supported by TEM characterization.

In summary, through surface modification and nano-micro structure, large thermal conductivity of 0.808 W m^{-1} K^{-1} (4.3 times that of epoxy) is obtained at 50 wt% content, which is equal to 26.5% in volume fraction.

Thermal stability is important for polymer materials and the introduction of fillers may change thermal characteristics of resulting composites. Herein, thermal gravimetric analysis (TGA) is applied to measure thermal stability at a heating rate of 20 °C min^{-1} under N_2. **Fig. 9** shows TGA and DTG curves of neat epoxy and its composites at 10 wt% filler loading. Temperatures at 10, 50 % weight losses and maximum degradation rate are selected as feature parameters and summarized in **Table 1**. It`s observed that within tested range, all samples display similar degradation profile, suggesting the addition of fillers doesn`t alter degradation mechanism for epoxy composites. $T_{10\%}$, $T_{50\%}$ and T_{max} of neat epoxy are 354.59, 375.96 and 374.89 °C, respectively. As for composites, feature temperatures follow Epoxy/BN-HBP < Epoxy/BA-HBP(4:1) < Epoxy/Al_2O_3-HBP order. The addition of Al_2O_3-HBP particles remarkably improves thermal stability with $T_{10\%}$, $T_{50\%}$ and T_{max} increased by 8.43 °C, 14.31 °C and 15.09 °C, respectively. Two factors can be attributed to the enhancement in thermal degradation temperature: (1) ceramic fillers in composites can form isolation layers as mass transport barriers between matrix and surface where combustion occurs[26]; (2) thermal motion of chain segments is restricted due to covalent interface formed by reaction between amino groups in modified fillers and epoxide groups in matrix. However, for Epoxy/BN-HBP, feature temperatures are raised by 2.43, 6.43 and 1.12 °C, separately, not so apparent as Epoxy/Al_2O_3-HBP. This could be caused by the weak affinity between basal planes of BN-HBP and epoxy due to insufficient surface modification. Thereby, thermal degradation is inclined to start from these weak sites. In case of Epoxy/BA-HBP(4:1) with hybrid fillers, though $T_{10\%}$, $T_{50\%}$ and T_{max} raise by 4.92, 9.40 and 4.78 °C relative to neat epoxy, no obvious synergistic behavior is observed. To be noticed, the introduction of as received Al_2O_3 and BN will reduce thermal stability as is proved in previous work[27, 28]. In other words, surface modification with hyperbranched aromatic polyamide in this work can increase thermal stability. Differential Scanning Calorimetry (DSC) is conducted as shown in **Fig. S4** and similar results are observed.

2.4 Dielectric properties of epoxy nanocomposites

For polymer composites applied in high voltage fields, e.g., power cable terminations

and rotating machine windings, breakdown strength representing the ability to withstand electric fields is a crucial design parameter. In this paper, measured breakdown strength is further treated by a two-parameter Weibull statistical distribution written as[29]

$$P = 1 - \exp [- (E/E_0)^{\beta}] \quad (3)$$

where P is cumulative probability of electrical failure, E is experimental breakdown strength, E_0 is the characteristic breakdown strength at cumulative failure probability of 63.2% and is frequently used for comparison between different composites, β is shape parameter relative to scatter of the data. For failure probability, IEEE 930-2004 standard recommends a brief approximation:

$$Pi = (i - 0.44) / (n + 0.25) \times 100\% \quad (4)$$

where i is the i-th result when values of E are sorted in ascending order, n is number of samples and n = 15 in this work. To study the influence of surface modification and nano-micro structure on breakdown strength, neat epoxy and composites with individual BN-HBP, Al_2O_3-HBP or hybrid fillers at 10 wt% content (4.4 vol%) are investigated. Weibull plots are presented in **Fig. 10** with characteristic breakdown strength and shape parameter summarized in **Table 1**.

Breakdown strength is susceptible to factors such as sample thickness, temperature, frequency et al. and under our experiment condition, neat epoxy presents a characteristic breakdown strength of 33.38 kv mm^{-1}. It`s already known that the addition of untreated fillers, e.g. Al_2O_3, TiO_2, ZnO, into matrix will reduce electric resistance, since defects as voids and porosity are introduced in the meantime. These weak sites consisting of gas can incur local failure and promote treeing propagation[30]. However, Epoxy/BN-HBP and Epoxy/Al_2O_3-HBP with treated fillers in our work show raised breakdown strength of 34.77 and 36.95 kv mm^{-1}, respectively. This can be interpreted from the view of filler dispersion and interface interaction. Firstly, surface modification with hyperbranched aromatic polyamide endows fillers with favorable compatibility and better dispersion in the matrix (**Fig. 4,8**), which can lead to higher breakdown strength[31]. Secondly, HBP tethered to surfaces of both Al_2O_3 and BN reduce interface tension by forming covalent bonds between amino groups and epoxide groups in curing process. Strong interface can reduce defect quantity/size. This is also indicated by shape parameter, as larger β values

of Epoxy/BN-HBP (18.78) and Epoxy/Al_2O_3-HBP (19.62) than epoxy of 16.56 reflect a narrower data distribution of defects or fillers. Moreover, strong covalent interface can localize electrons, ions and polymer chains, which offers more stable potential energy states[32, 33]. In conclusion, surface modification is crucial to the increase of breakdown strength. To be noticed, E_0 of Epoxy/BN-HBP is higher than that of Epoxy/Al_2O_3-HBP and this can be attributed to ultrahigh intrinsic dielectric strength and large aspect ratio of *h*-BN[34].

For Epoxy/BA-HBP(4:1) with nano-micro structure of hybrid fillers, it`s interesting to observe an even higher breakdown strength of 40.55 kv mm^{-1}, which is 121.5% that of neat epoxy. We envisage nano-micro filler mixture can contribute to a more compact structure and raise encountering frequency between electrical treeing and fillers, which results in more tortuous paths for treeing propagation[35]. Besides, Al_2O_3-HBP particles may serve as physical barriers to hinder isolated BN-HBP platelets from stacking during blending and curing processes, indicating a more favorable dispersion for fillers. Also, it is reasonable to find a decrease in shape parameter of 17.08, since fillers with different dimensions and sizes are introduced at the same time. Finally, epoxy composites with high breakdown strength are prepared by surface treatment and nano-micro structure.

Frequency dependence of dielectric permittivity, ε` and loss tangent, tan δ for neat epoxy and its composites with modified fillers are also studied at room temperature as shown in **Fig. 11**. It is found that the introduction of individual Al_2O_3-HBP, BN-HBP or hybrid fillers at 10 wt% loading has no obvious influence on dielectric permittivity (around 3.5) and loss tangent (below 0.02) over tested frequency range. To be noticed, Epoxy/BA-HBP(4:1) with hybrid fillers shows the highest ε` of 4.58 over other samples at 10^4 Hz and tan δ remains low of 0.013. The mechanism is not clear so far and the result is within the range of experimental errors.

3. Conclusion

In this work, we prepared a series of epoxy composites with HBP grafted *h*-BN platelets and α-Al_2O_3 particles. It`s found that nano-micro structure of 2-D and 0-D hybrid fillers presents apparent synergistic effect on thermal conductivity and ac breakdown strength.

Besides, surface treatment contributes to improve thermal conductivity, thermal stability and breakdown strength. By structure design and surface treatment, Epoxy/BA-HBP(4:1) shows high thermal conductivity of 0.808 W $m^{-1} K^{-1}$ (4.3 times that of epoxy) at 26.4 vol% content. The breakdown strength of Epoxy/BA-HBP(4:1) with 4.4 vol% fillers is up to 40.55 kv mm^{-1}, 21.5% higher than that of epoxy (33.38 kv mm^{-1}). The approach described provides a route for preparing composites with high thermal conductivity and breakdown strength at low content, which is especially critical for high output electrical equipment. Also, our findings offer a better understanding of interface and synergistic effect for composites with 2-D and 0-D hybrid modified fillers.

Acknowledgements

The authors gratefully acknowledge supports from the National Science Foundation of China (No. 51107081, 51277117), the Special Fund of National Priority Basic Research of China (No. 2014CB239503) and Shanghai Leading Academic Discipline Project (No. B202). The authors are also grateful to researchers in the instrument analysis center of Shanghai Jiao Tong University for their help in material analysis.

Reference

[1] B. A. Rozenberg, R. Tenne, Prog. Polym. Sci. **2008**; 33, 40.

[2] R. Prasher, P. IEEE. **2006**; 94, 1571.

[3] R. Qian, J. Yu, C. Wu, RSC Adv.. **2013**; 3, 17373.

[4] Z. Han, A. Fina, Prog. Polym. Sci. **2011**; 36, 914.

[5] C. Min, D. Yu, J. Cao, Carbon. **2013**; 55, 116.

[6] X. Huang, X. Qi, F. Boey, Chem. Soc. Rev. **2012**; 41, 666.

[7] T. Li, S. L. Hsu, J. Phys. Chem. B. **2010**; 114, 6825.

[8] M. Harada, N. Hamaura, M. Ochi, Compos. Part B-Eng. **2013**; 55, 306.

[9] W. Peng, X. Huang, J. Yu, Compos. Part A -Appl. S. **2010**; 41, 1201.

[10] S. Gupta, P. C. Ramamurthy, G. Madras, Polym. Chem. **2011**; 2, 221.

[11] S. Zhao, L. Schadler, R. Duncan, Compos. Sci. Techno. **2008**; 68, 2965.

[12] P. L. Teh, M. Jaafar, H. M. Akil, Polym. Adv. Techno. **2008**; 19, 308.

[13] Z. Li, K. Okamoto, Y. Ohki, IEEE T. Dielect. El. In. **2010**; 17, 653.

[14] I. Jo, M. T. Pettes, J. Kim, Nano Lett. **2013**; 13, 550.

[15] G.-H. Lee, Y.-J. Yu, C. Lee, Appl. Phys. Lett. **2011**; 99, 243114.

[16] A. K. Roy, B. L. Farmer, V. Varshney, App. Mater. Interfaces. **2012**; 4, 545.

[17] X. Huang, T. Iizuka, P. Jiang, J. Phys. Chem. C. **2012**; 116, 13629.

[18] X. Xiao, S. Lu, B. Qi, RSC Adv. **DOI: 10.1039/c0xx00000x**.

[19] C. Zhi, Y. Bando, C. Tang, Adv. Mater. **2009**; 21, 2889.

[20] S. P. YL Zhao, Macromolecules. **2007**; 40, 9116.

[21] K. Sato, H. Horibe, T. Shirai, J. Mater. Chem. **2010**; 20, 2749.

[22] S. Lu, S. Li, J. Yu, RSC Adv.. **2013**; 3, 8915.

[23] L. M. McGrath, R. S. Parnas, S. H. King, Polymer. **2008**; 49, 999.

[24] S. Choi, H. Im, J. Kim, Compos. Part A -Appl. S. **2012**; 43, 1860.

[25] S.-Y. Yang, C.-C. M. Ma, C.-C. Teng, Carbon. **2010**; 48, 592.

[26] Y. S. Ye, Y. C. Yen, C. C. Cheng, Polymer. **2010**; 51, 430.

[27] J. Yu, X. Huang, C. Wu, Polymer. **2012**; 53, 471.

[28] J. Yu, X. Huang, L. Wang, Polym. Chem. **2011**; 2, 1380.

[29] Y. Z. Xingyi Huang, Pingkai Jiang, IEEE T. Dielect. El. In. **2010**; 17, 635.

[30] S. Singha, M. J. Thomas, IEEE T. Dielect. El. In. **2008**; 15, 12.

[31] X. Huang, Y. Zheng, P. Jiang, IEEE T. Dielect. El. In. **2010**; 17, 635

[32] T. P. Schuman, S. Siddabattuni, O. Cox, Compos. Interfaces. **2011**; 17, 719.

[33] P. Preetha, M. J. Thomas, IEEE T. Dielect. El. In. **2011**; 18, 1526.

[34] Y. Song, Y. Shen, H. Liu, J. Mater. Chem. **2012**; 22, 16491.

[35] T. Imai, F. Sawa, T. Nakano, IEEE T. Dielect. El. In. **2006**; 13, 319

Table 1. weight loss temperature T, characteristic breakdown strength E_0 and shape parameter β of neat epoxy and its composites with 10 wt% individual or hybrid fillers

	Weight loss temperature /°C			Breakdown performance	
	$T_{10\%}$	$T_{50\%}$	T_{max}	E_0 (kv mm^{-1})	β
Neat epoxy	354.59	375.96	374.89	33.38	16.56
Epoxy/BN-HBP	357.02	382.39	376.01	36.95	18.78
Epoxy/BA-HBP(4:1)	359.51	385.36	379.67	40.55	17.08
Epoxy/Al_2O_3-HBP	363.02	390.27	389.98	34.77	19.62

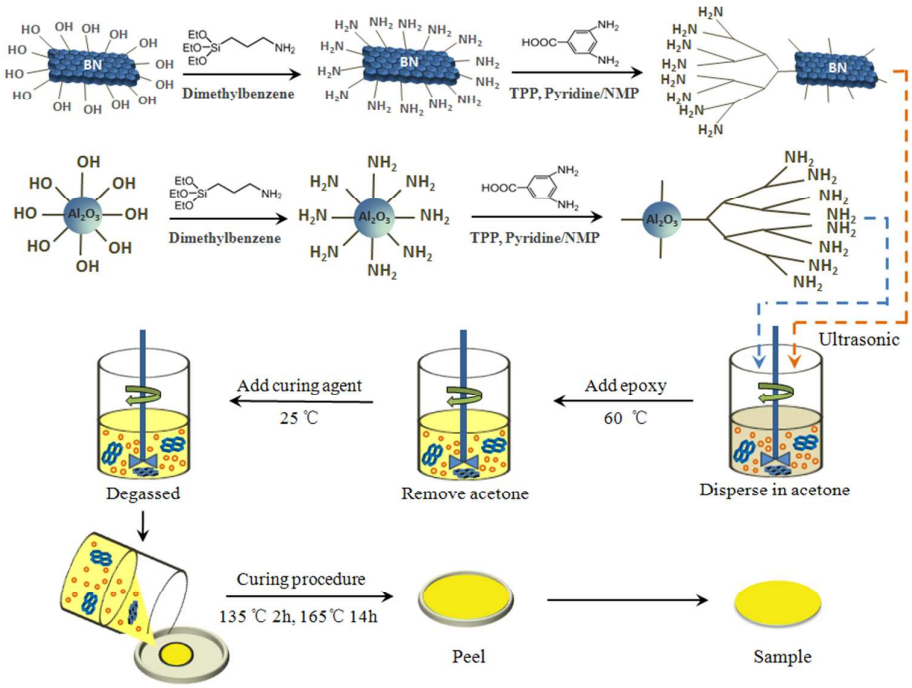

Fig. 1. An illustration for the preparation process of epoxy composites

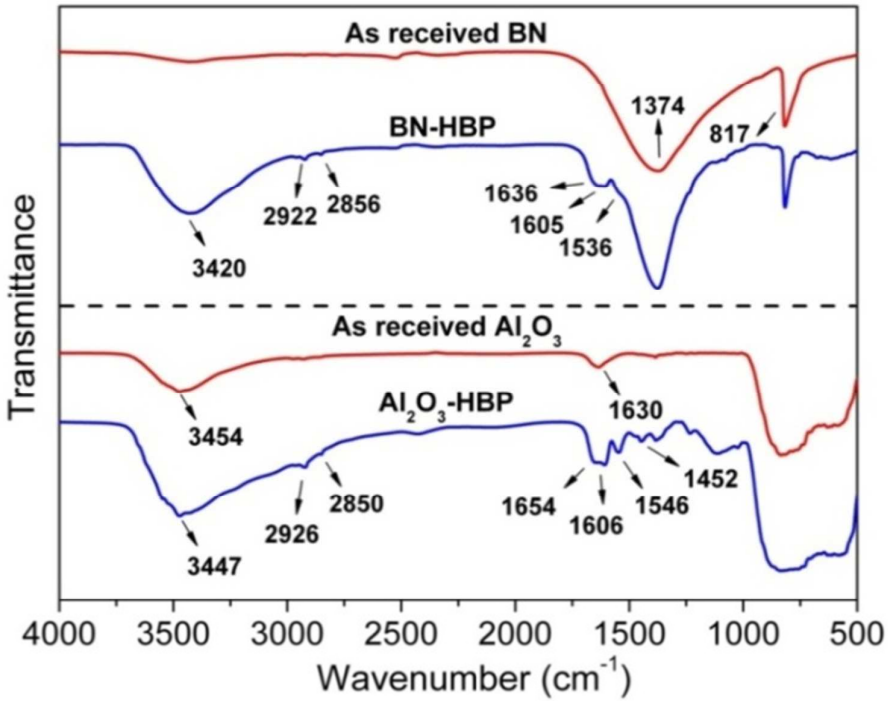

Fig. 2. FT-IR spectra of as received BN, BN-HBP, as received Al_2O_3 and Al_2O_3-HBP

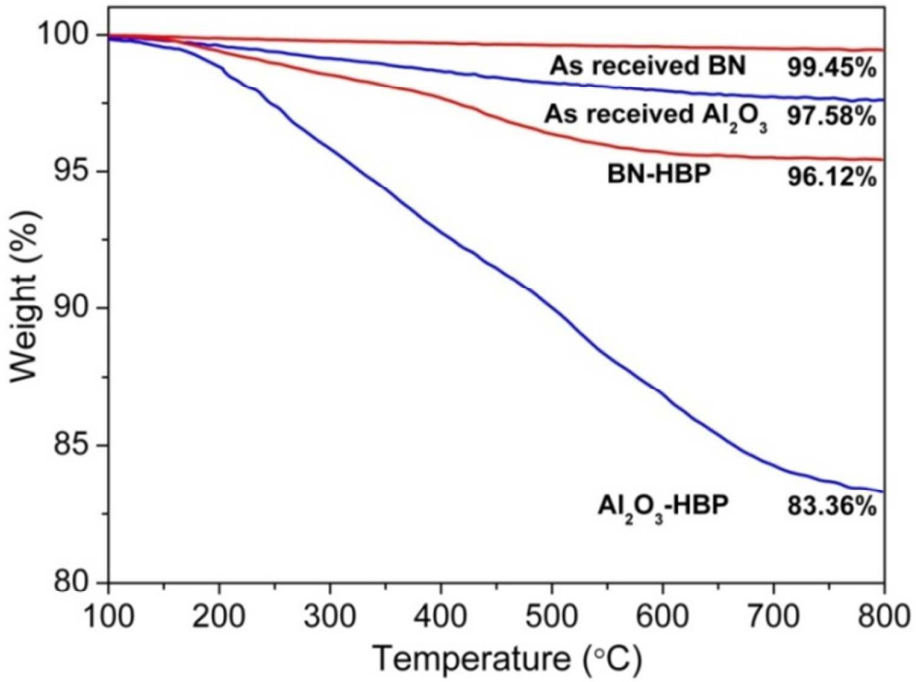

Fig. 3. TGA curves of as received BN, BN-HBP, as received Al_2O_3 and Al_2O_3-HBP recorded under nitrogen

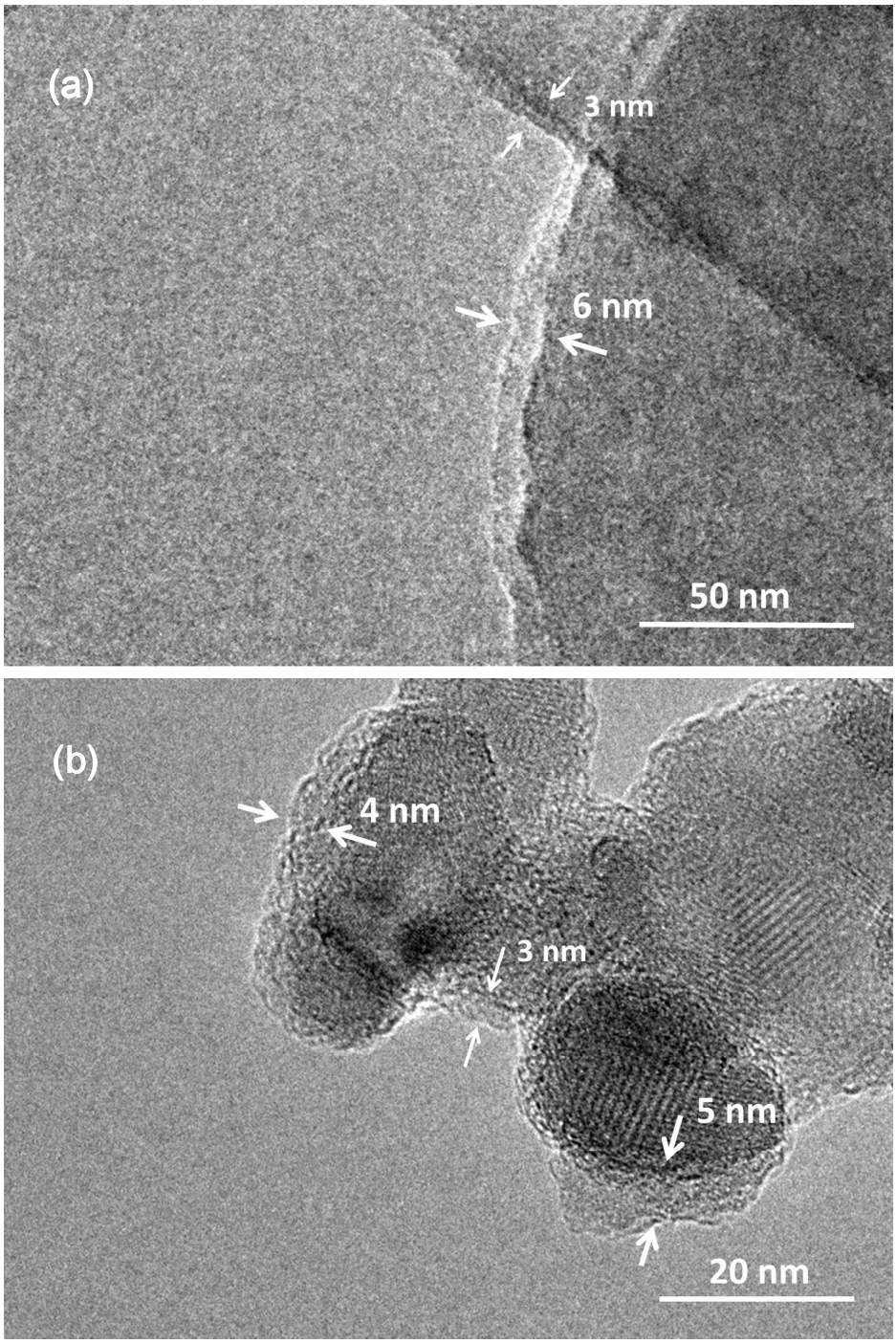

Fig. 4. TEM images of functionalized fillers: (a) BN-HBP, (b) Al_2O_3-HBP

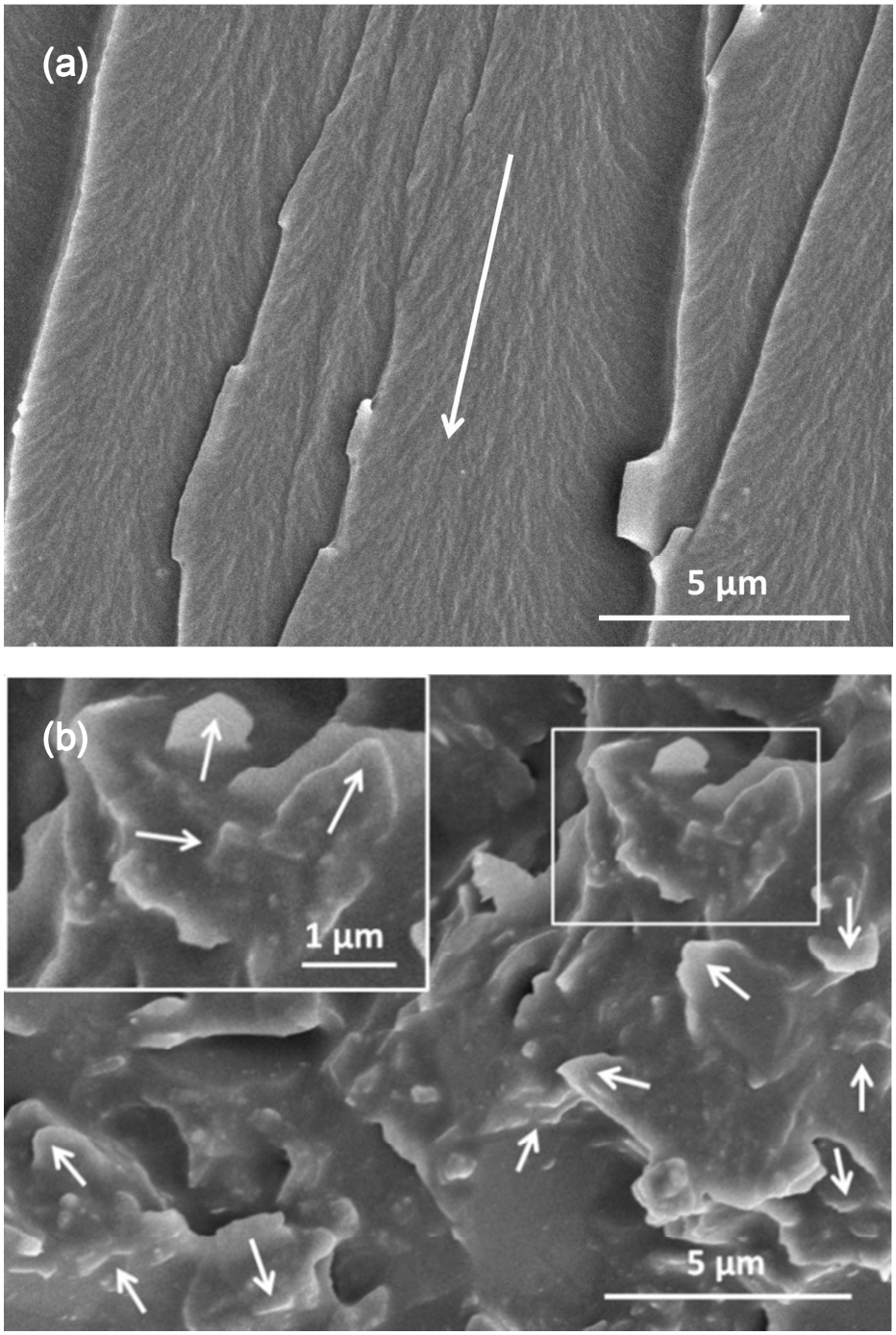

Fig. 5. SEM images of fracture surfaces: (a) neat epoxy; (b) 10 wt% loaded composite with 80 wt% BH-HBP in hybrid filler, inset: an enlarged view of the framed region

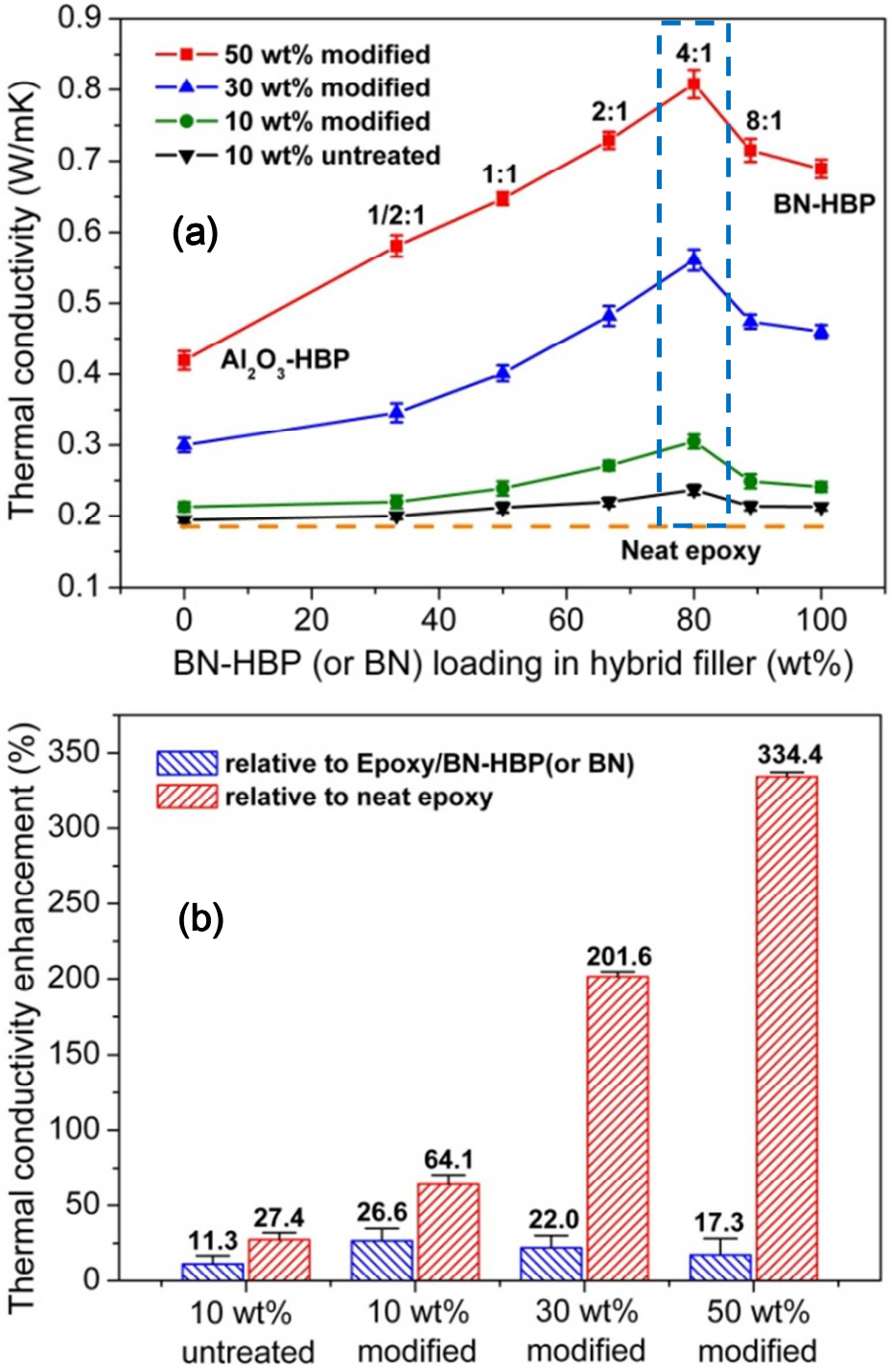

Fig. 6. (a) Thermal conductivity of epoxy composites as a function of BN-HBP (or BN) loading in hybrid filler at filler loading from 10 to 30 wt%; thermal conductivity of neat epoxy is marked by the dash line; (b) thermal conductivity enhancement of composites framed in (a) relative to neat epoxy and Epoxy/BN-HBP (or BN)

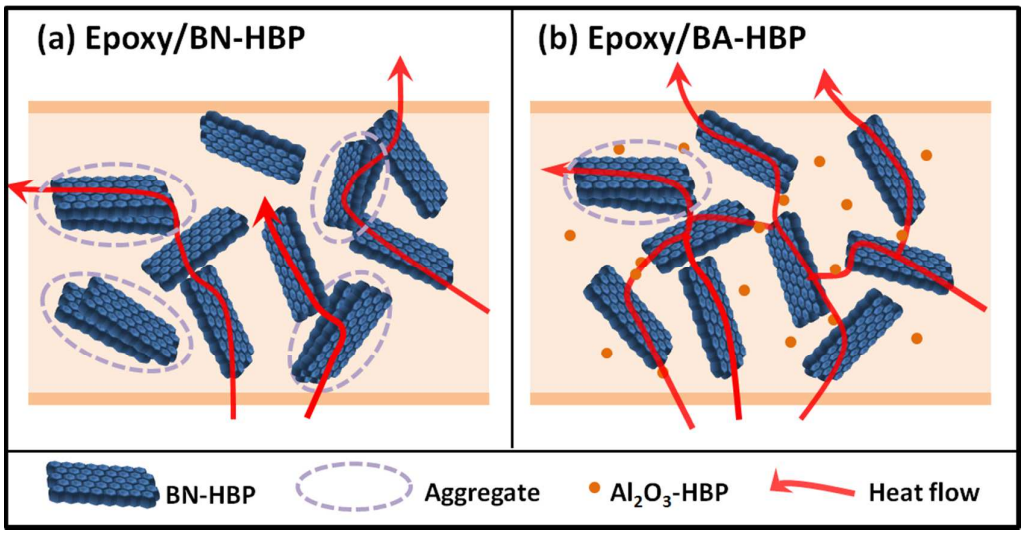

Fig. 7. composite models with (a) individual BN-HBP platelets and (b) hybrid fillers

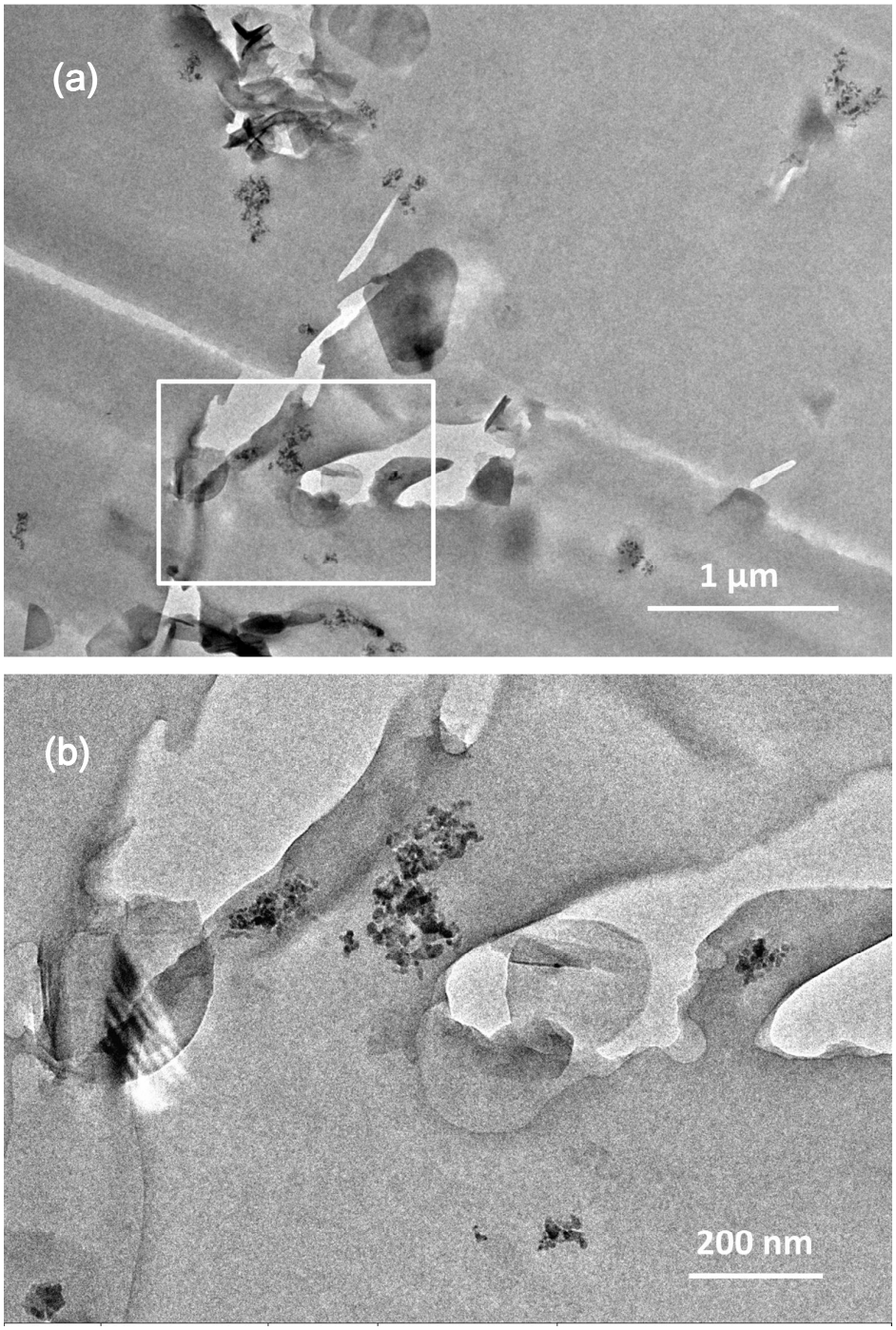

Fig. 8. TEM image of (a) Epoxy/BA-HBP(4:1) with 10 wt% total filler loading and (b) an enlarged view of the framed region

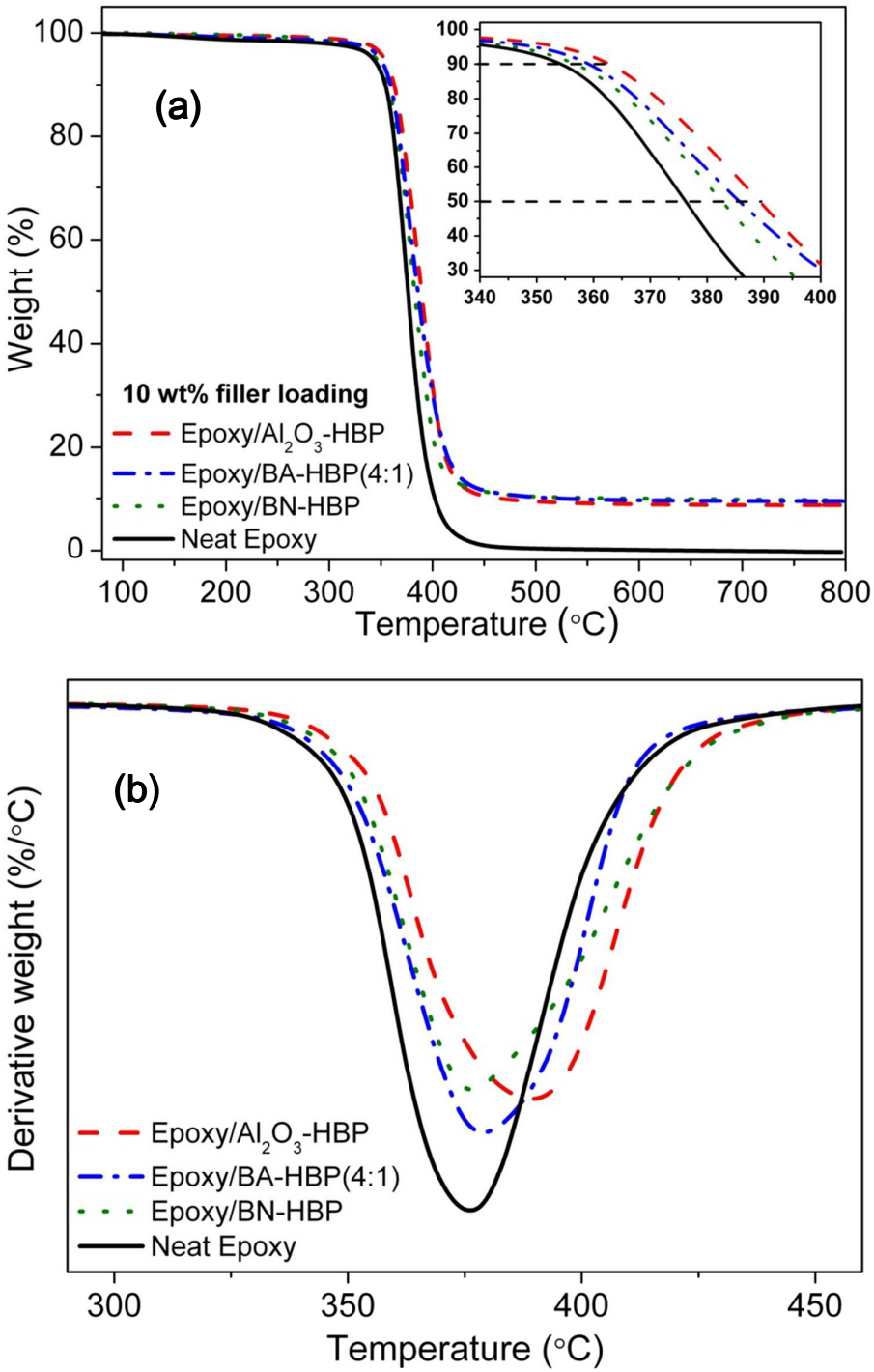

Fig. 9. TGA (a) and DTG (b) curves of neat epoxy and its composites at filler loading of 10 wt%; inset: an enlarged view of TGA curves from 340 °C to 400 °C

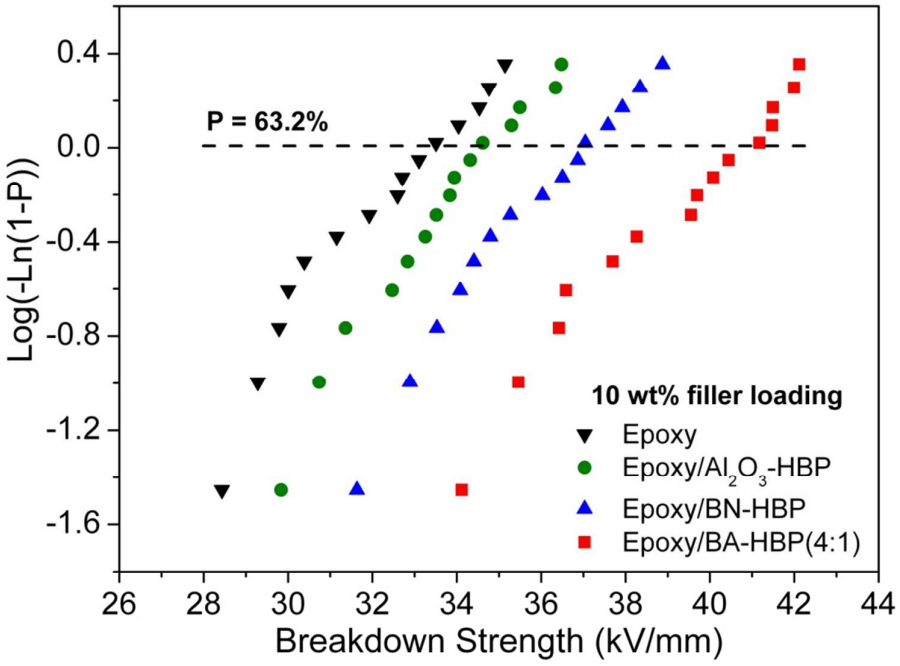

Fig. 10. Weibull plots of breakdown strength for neat epoxy and its composites with individual or hybrid fillers at total loading of 10 wt%

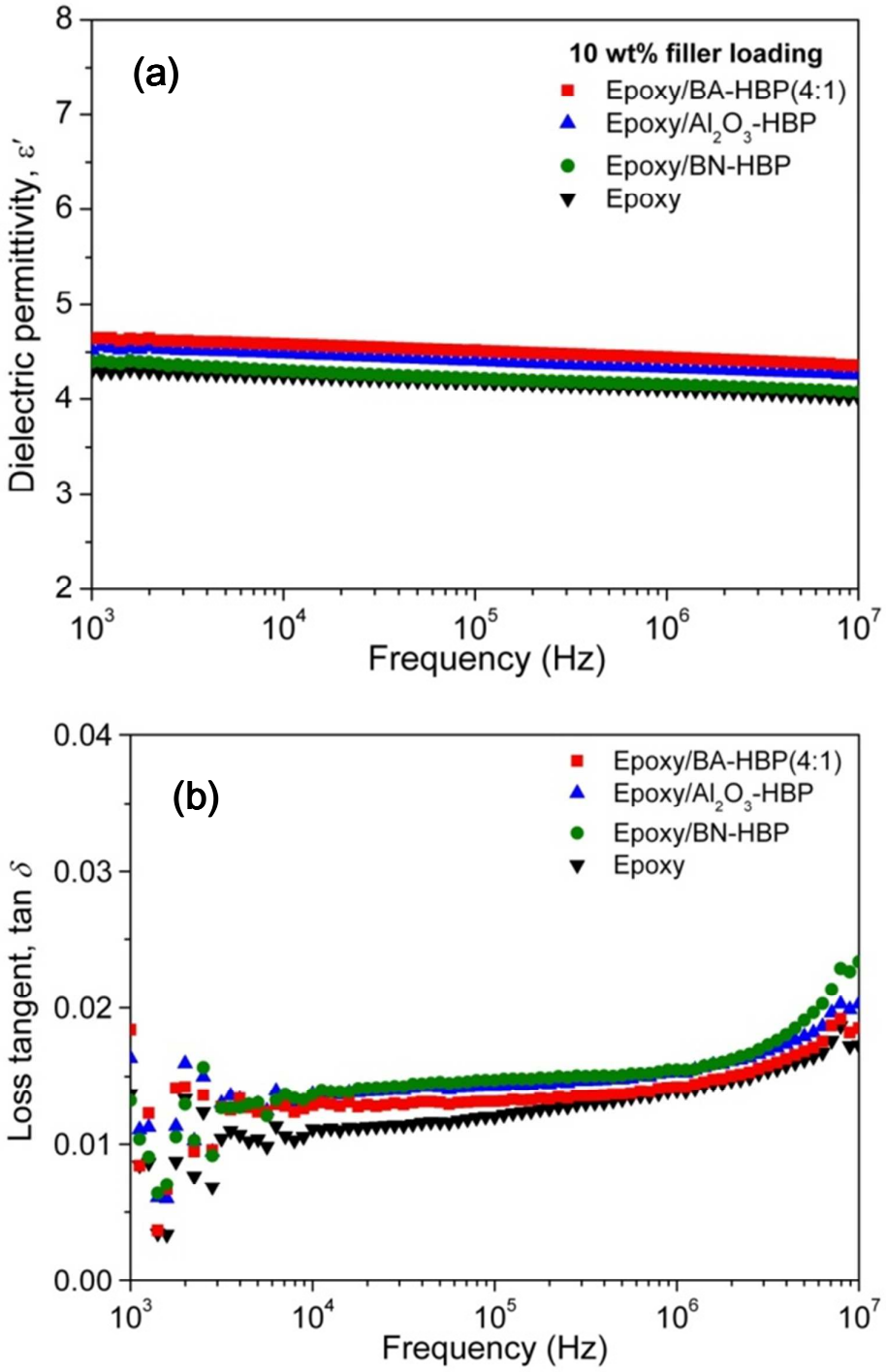

Fig. 11. Frequency dependence of (a) dielectric permittivity, ε`, (b) loss tangent, tan δ for neat epoxy and 10 wt% loaded epoxy composites with individual or hybrid fillers from 10^3 Hz to 10^7 Hz at room temperature